A Novel Methodology for Predicting Critical Salt Concentration of Bubble Coalescence Inhibition

Mahshid Firouzi and Anh V. Nguyen*

School of Chemical Engineering

The University of Queensland, Brisbane, Queensland 4072, Australia

ABSTRACT

Bubble coalescence in some salt solutions can be inhibited if the salt concentration reaches a critical concentration C_{cr}. There are three models available for C_{cr} in the literature, but fail to predict C_{cr} correctly. The first two models employ the van der Waals attraction power laws to establish C_{cr} from the discriminant of quadratic or cubic polynomials. To improve the two models, the third model uses the same momentum balance equation of the previous models, but different intermolecular force generated by water hydration with exponential decaying. The third prediction for C_{cr} requires the experimental input for film rupture thickness and is incomplete. We show further in this paper that the third model is incorrect. We propose a novel methodology for determining C_{cr} which resolves the mathematical uncertainties in modelling C_{cr} and can explicitly predict it from any relevant intermolecular forces. The methodology is based on the discovery that C_{cr} occurs at the local maximum of the balance equation for the capillary pressure, disjoining pressure and pressure of the Gibbs-Marangoni stress. The novel generic approach is successfully validated using non-linear equations for complicated disjoining pressure.

KEYWORDS: saline water, Gibbs-Marangoni effect, disjoining pressure, van der Waals attractions, electrical double-layer interactions

1. INTRODUCTION

Inorganic salts are known to significantly influence bubble coalescence in liquids, bubble size and distribution, gas holdup, gas-liquid interfacial area and bubble rise velocity, all of which critically govern many important devices (e.g., bubble columns, distillation towers and bioreactors) and industrial processes (e.g., dissolved air flotation used to prepare seawater fed to desalination plants, and induced air flotation used to recover valuable minerals from the earth's crust) [1-9]. The foaminess of ocean waves on the beach exemplifies the significant effect of salts in reducing bubble coalescence in nature. The experiments show that bubble coalescence can be significantly inhibited beyond a critical salt concentration, C_{cr} (also termed the transition concentration) [5, 9-14]. It is referred to as the critical concentration here because bubbles and liquid films undergo a transition from coalescence to non-coalescence at the critical moment when the opposing forces are balanced.

Despite the maturity of experimental techniques and evidence, a full theoretical understanding of inhibition of bubble coalescence in salt solutions is still lacking. So far, there are three models available in the literature to predict the critical salt concentrations[15-17]. All of these models are based on the finding that at C_{cr}, salts can alter the interfaces of the intervening liquid films between bubbles, such that they change from mobile interfaces at low salt concentration to the immobile interfaces at high salt concentration [&]. Consequently, at C_{cr} the film drainage changes from the inertial regime at low salt concentration to the viscous regime at high salt concentration [16-19]. At the transition from the inertial to viscous drainage regime, the pressure of the Gibbs-Marangoni stress can be sufficiently large to counterbalance the driving force of film rupture by the capillary pressure and attractive disjoining pressure. For example, Marrucci [15] considered the London-van der Waals attraction in the pressure balance, and the corresponding expression for C_{cr} is obtained from the discriminant of the cubic polynomial as follows [16]:

$$C_{cr} = 0.084\upsilon R_g T \left(\frac{\sigma A^2}{R}\right)^{1/3} \left(\frac{\partial \sigma}{\partial C}\right)^{-2} \qquad [1]$$

where υ is the number of ions produced upon salt dissociation, R_g is the gas constant, T is the absolute temperature, A is the non-retarded Hamaker constant, R is the bubble radius, and σ and $\partial\sigma / \partial C$ are the surface tension and the surface tension gradient with respect to salt concentration, respectively.

Although the electromagnetically non-retarded London-van der Waals attraction is strong, it is very short-ranged, i.e., shorter than 10 nm, while gas bubbles in saline water normally coalesce at the film thickness larger than 40 nm. Therefore, it is argued that the electromagnetically retarded Casimir-van der Waals attraction acting over the distance of the rupture thickness of the film should be used in modelling the critical salt concentration [16]. The quadratic polynomial of the modified theory gives the following prediction for C_{cr} [16]:

$$C_{cr} = 0.707 \upsilon R_g T \left(\frac{\sigma B}{R} \right)^{1/2} \left(\frac{\partial \sigma}{\partial C} \right)^{-2} \qquad [2]$$

where B is the retarded Hamaker constant. The authors also examined the effect of inertial drainage on C_{cr}, obtaining another prediction similar to Eq. [2], where the numerical constant is replaced by 1.181. It is noted that an exact value for the Hamaker constants in Eqs. [1] and [2] is difficult to determine. Indeed, using the advanced Lifshitz theory on van der Waals interaction energy we have recently shown [20] that the Hamaker constants were not correctly calculated by previous authors and both Eqs. [1] and [2] under-estimate the experimental results for C_{cr}.

In 2005, Chan and Tsang [17] were not able to compare the two models for C_{cr} with their experimental results and modified the previous models by replacing the van der Waals attractions by the repulsive hydration forces. They argued that the Gibbs-Marangoni tangential stress produced by the surface tension gradient would not be strong enough to inhibit the bubble coalescence. Their prediction for C_{cr} is a function of the thickness of the film at rupture, h_{rup}, as follows:

$$C_{cr} = \upsilon R_g T \left(\frac{\sigma h_{rup}^2}{2R} \right) \left(\frac{\partial \sigma}{\partial C} \right)^{-2} \qquad [3]$$

Since the film rupture thickness is usually unknown, the third model requires further experimental work to determine the thickness as the model input. The third model is incomplete because C_{cr} can usually be obtained using simple devices like a bubble column [9] and independent measurements of film rupture thickness are not required. We show below that this model is also incorrect.

In this paper, we present a new, generic method for predicting C_{cr} from the same starting equation of momentum balance for liquid flow inside thin films. This method resolves the mathematical uncertainties and incorrectness in modelling C_{cr} and can be used with complicated equations for intermolecular forces which likely play the key role in the bubble coalescence affair. Indeed, the failure of the third model is due to the fact that the proposed pressure balance equation cannot be broken down at the transition, which can be proved by using the new methodology. The outcome of our novel approach is the ability to explicitly predict C_{cr} from the known surface tension of salt solutions and its concentration gradient, and the physical properties of air bubbles such as size and intermolecular forces.

2. MODEL DEVELOPMENT

The starting point of many modelling works in the area of bubble coalescence and thin liquid film drainage is the momentum balance as described by the Navier-Stokes equation for low Reynolds number flows within thin liquid films. This is a well-established area, known as the lubrication theory. Therefore, we do not repeat all the derivations here and consider the available generic result for pressure balance equation at the transition [16-17]:

$$\frac{4C}{h^2 \upsilon R_g T}\left(\frac{\partial \sigma}{\partial C}\right)^2 - \frac{2\sigma}{R} + \Pi(h) = 0 \qquad [4]$$

where $\Pi(h)$ is the disjoining pressure of intermolecular forces between the film surfaces, h is the averaged film thickness, the first term is the pressure of the Gibbs-Marangoni stress and the second term is the capillary pressure. In Eq. [4], the inertial effect on the film drainage is ignored.

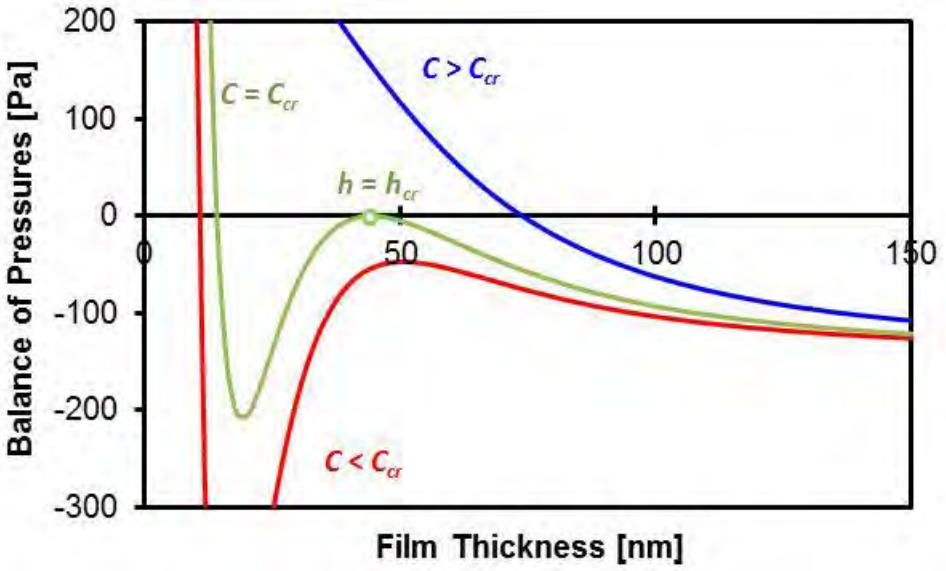

Figure 1. Variation of balance of pressures as described by the left hand side of Eq. [4] versus film thickness at three characteristic salt concentrations, i.e., low concentration ($C < C_{cr}$), high concentration ($C > C_{cr}$) and critical concentration ($C = C_{cr}$). The model parameters include: $R = 0.001$ m, $\nu = 2$, $\Pi(h) = -10000 \times \exp(-h/10)$ [Pa], $C_{cr} = 0.000629$ M, $T = 293$ K, $\sigma = 0.072$ N and $\partial\sigma / \partial C = 0.001\ \mathrm{N \cdot m^{-1} \cdot M^{-1}}$.

Now the new modelling approach is developed based on the following analysis of Eq. [4] and discovery. It is noted that when h is very large, the Gibbs-Marangoni pressure (first term) and the disjoining pressure (third term) of Eq. [4] approach zero, and the balance of pressures on the left hand side of Eq. [4] becomes negative (i.e., is equal to $-2\sigma / R$). Likewise as h approaches zero $1/h^2$ approaches infinity, and the balance of pressures becomes a large positive value. For intermediate values of film thickness, $10\ \mathrm{nm} < h < 100\ \mathrm{nm}$, the change in the balance of pressures depends to a significant extent on the variation of the disjoining pressure versus h as well as the salt concentration. For example, for a low salt concentration and an attractive (negative) disjoining pressure, the balance of pressures can increase from the negative value of $-2\sigma / R$ to a local maximum, pass through a local minimum and then increase to a large positive value (infinity) when the film thickness h decreases from a very large value (infinity) to a small value (zero). Shown in Figure 1 is the typical variation of the balance of pressures on the left hand side of Eq. [4] versus

the film thickness and salt concentration. Without loss of generality, a single exponential dependence of the attractive disjoining pressure on the film thickness, i.e., $\Pi = -A\exp\left(-h/\lambda\right)$, is used for the illustration in Figure 1. If the salt concentration is high, the balance of pressures does not exhibit any local maximum or minimum, i.e., it increases monotonically from the negative value of $-2\sigma/R$ (at $h \to \infty$) to $+\infty$ (at $h \to 0$) as shown in Figure 1.

The variation of the balance of pressures as illustrated in Figure 1, in conjunction with the available experimental observations, is important for our interpretation of the stability of aqueous films of salt solutions. Firstly, the aqueous films of salt solutions (surfactant-free films) are relatively thick and often rupture before becoming a very thin film of a thickness less than 20 nm. For those films of low salt concentrations ($C < C_{cr}$), the balance of pressures is negative and, therefore, Eq. [4] cannot be satisfied, i.e., it has no real solution for *h*. This nonexistence of a solution for *h* means that a (meta-) stable or (quasi-) equilibrated film cannot exist under the condition of low salt concentration. For high salt concentrations ($C > C_{cr}$), Eq. [4] can be satisfied, i.e., it has a real solution for *h* for the film stability, which is the horizontal coordinate of the intercept of the blue curve in Figure 1 with the horizontal axis – the existence of the solution for *h* means that a (meta-) stable or (quasi-) equilibrated film exists under the condition of high salt concentration. Critically, the transition from unstable to stable films occurs when Eq. [4] is just met, i.e., the curve of the balance of pressures just locally touches the horizontal axis as illustrated by the green curve in Figure 1. This condition can happen when the local maximum is equal to zero and can mathematically be described as follows:

$$\frac{4C_{cr}}{{h_{cr}}^2 \upsilon R_g T}\left(\frac{\partial\sigma}{\partial C}\right)^2_{C=C_{cr}} - \frac{2\sigma}{R} + \Pi\left(h_{cr}\right) = 0 \qquad [5]$$

$$-\frac{8C_{cr}}{{h_{cr}}^3 \upsilon R_g T}\left(\frac{\partial\sigma}{\partial C}\right)^2_{C=C_{cr}} + \Pi'\left(h_{cr}\right) = 0 \qquad [6]$$

$$\frac{24C_{cr}}{h_{cr}{}^4 \upsilon R_g T}\left(\frac{\partial \sigma}{\partial C}\right)^2_{C=C_{cr}} + \Pi''(h_{cr}) < 0 \qquad [7]$$

where h_{cr} is the (critical) thickness of the transition from its instability to stability , and the single or double primes describe the first and second derivatives of the disjoining pressure with respect to *h*. Equations [6] and [7] describe the position of the local maximum while Eq. [5] describes the condition where the value of the local maximum is equal to zero.

Equations [5] and [6] can be simultaneously solved for C_{cr} and h_{cr}. Mathematically, the two equations describe the necessary condition for finding a solution for C_{cr} and h_{cr}, while Eq. [7] is a sufficient condition for the local maximum to occur. Eqs. [6] and [7] have not been established previously. If Eq. [6] is not used, the solution of Eq. [5] for C_{cr} is uncertain because h_{cr} is unknown and many pairs of numerical values for C_{cr} and h_{cr} can be found to satisfy Eq. [5]. This is the critical point of the previous papers [15, 17] which require experimental data for h_{cr} to remove the mathematical uncertainty. Eq. [7] provide a quick and helpful check whether or not a solution for C_{cr} exists mathematically. Indeed, the third modelling approach taken by Chan and Tsang [17] fails to satisfy Eq. [7] and is proved to be incorrect as described in the following section.

3. FURTHUR EVALUATIONS AND APPLICATIONS

Equations [5] to [7] present the new model prediction for determining C_{cr}. The new model also allows for the prediction of the critical film thickness, h_{cr}, of the transition from instability to stability of saline water film drainage or vice versa. The model is generic because it can be used *i*) to predict C_{cr} when a complicated/nonlinear isotherm for the disjoining pressure is employed, and *ii*) to establish the simple solutions for C_{cr} which were previously obtained from different simple models, such as those described by Eqs. [1] and [2]. The details are shown below.

When the non-retarded van der Waals disjoining pressure, $\Pi = -A/6\pi h^3$ (here the non-retarded Hamaker constant, A, is a positive number), is used, Eqs. [5] to [7] gives

$$\frac{4C_{cr}}{h_{cr}{}^2 \upsilon R_g T}\left(\frac{\partial\sigma}{\partial C}\right)^2_{C=C_{cr}} - \frac{2\sigma}{R} - \frac{A}{6\pi h_{cr}{}^3} = 0 \qquad [8]$$

$$-\frac{8C_{cr}}{h_{cr}{}^3 \upsilon R_g T}\left(\frac{\partial\sigma}{\partial C}\right)^2_{C=C_{cr}} + \frac{A}{2\pi h_{cr}{}^4} = 0 \qquad [9]$$

$$\frac{24C_{cr}}{h_{cr}{}^4 \upsilon R_g T}\left(\frac{\partial\sigma}{\partial C}\right)^2_{C=C_{cr}} - \frac{2A}{\pi h_{cr}{}^5} < 0 \qquad [10]$$

Solving these equations for the critical salt concentration and film thickness yields

$$C_{cr} = \left(\frac{3}{512\pi^2}\right)^{1/3} \upsilon R_g T \left(\frac{A^2\sigma}{R}\right)^{1/3} \left(\frac{\partial\sigma}{\partial C}\right)^{-2}_{C=C_{cr}} \qquad [11]$$

$$h_{cr} = \left(\frac{AR}{24\pi\sigma}\right)^{1/3} \qquad [12]$$

$$-\left(\frac{3A^2\sigma}{R\pi^2}\right)^{1/3} < 0 \qquad [13]$$

Equation [11] is identical to Eq. [1] and the inequality [13] is automatically met, confirming the validity of the new model.

Likewise, for the retarded van der Waals disjoining pressure, $\Pi = -B/h^4$, solving Eqs. [5] to [7] yields

$$C_{cr} = \upsilon R_g T \left(\frac{B\sigma}{2R}\right)^{1/2} \left(\frac{\partial\sigma}{\partial C}\right)^{-2}_{C=C_{cr}} \qquad [14]$$

$$h_{cr} = \left(\frac{BR}{2\sigma}\right)^{1/4} \qquad [15]$$

$$-16\left(\frac{\sigma B}{2R}\right)^{1/2} < 0 \qquad [16]$$

Again, Eq. [14] is identical to Eq. [2] and the inequality [16] is automatically met, validating the new model again.

Finally, when the repulsive hydration disjoining pressure, $\Pi = (W/\lambda)\exp(-h/\lambda)$, as proposed by Chan and Tsang [17] is used, inserting the hydration disjoining pressure into Eqs. [5] to [7] gives

$$\frac{4C_{cr}}{{h_{cr}}^2 \upsilon R_g T}\left(\frac{\partial\sigma}{\partial C}\right)^2_{C=C_{cr}} - \frac{2\sigma}{R} + \frac{W}{\lambda}\exp\left(-\frac{h_{cr}}{\lambda}\right) = 0 \qquad [17]$$

$$-\frac{8C_{cr}}{{h_{cr}}^3 \upsilon R_g T}\left(\frac{\partial\sigma}{\partial C}\right)^2_{C=C_{cr}} - \frac{W}{\lambda^2}\exp\left(-\frac{h_{cr}}{\lambda}\right) = 0 \qquad [18]$$

$$\frac{24C_{cr}}{{h_{cr}}^4 \upsilon R_g T}\left(\frac{\partial\sigma}{\partial C}\right)^2_{C=C_{cr}} + \frac{W}{\lambda^3}\exp\left(-\frac{h_{cr}}{\lambda}\right) < 0 \qquad [19]$$

where W is the pre-exponential (force) constant (positive) and λ is the decay length of the hydration force. Since the left hand side of Eq. [18] is always negative and inequation [19] is always positive, Eq. [18] and inequation [19] cannot be satisfied by any real values of the salt concentration and film thickness, and therefore no real solutions for C_{cr} and h_{cr} can be found from Eqs. [17] to [19]. As a result, the proposal by Chan and Tsang [17] to replace the van der Waals attractions by the repulsive hydration forces is physically inconsistent and cannot be justified (The hydration force is also very short range, i.e., the decay length of the hydration force is shorter than 2 nm [21-25] and cannot inhibit film rupture between two bubbles which occurs when the thickness is significantly larger than 2 nm).

Likewise, not only the repulsive hydration disjoining pressure, but any other (single or combined) repulsive disjoining pressure cannot be the main driving force for inhibiting the bubble

coalescence in salt solutions. This is because in the case of the repulsive disjoining pressure being a decreasing function of the film thickness, first derivative of the pressure term in Eq. [6] is negative and the left hand side of Eq. [6] is negative, making Eq. [6] unsolvable mathematically. In the other cases, when a single repulsive disjoining pressure together with another attractive disjoining pressure provides a combined (summed) disjoining pressure with its first derivative being positive, Eq. [6] can be satisfied and a mathematical solution to the new model Eqs. [5] to [7] can be found. This case is demonstrated in the following.

In many cases, the disjoining pressure can have a number of components with compatible magnitudes at compatible separation distances, e.g., the van der Waals pressure and the electric double-layer pressure at relatively high salt concentrations. No model for C_{cr} in these complicated cases is available in the literature. Here we show that the new model proposed in this paper can be used with the complicated/nonlinear disjoining pressure. We consider the disjoining pressure as a sum of the retarded van der Waal interaction and the electrical double-layer interaction, i.e.,

$$\Pi(h) = -\frac{B}{h^4} + 64000CR_gT\tanh^2\left(\frac{z\psi F}{4R_gT}\right)\exp(-\kappa h) \qquad [20]$$

where F is the Faraday constant, z is the ion valence of the symmetric z:z salt and ψ is the potential of the air-salt solution interface. The Debye constant is defined as

$$\kappa = \left\{\frac{2000CF^2z^2}{\varepsilon\varepsilon_0 R_gT}\right\}^{1/2} \qquad [21]$$

where ε and ε_0 are the dielectric constants of the vacuum and water permittivity, respectively. In Eq. [20], the superposition approximation for the double-layer interaction [1] is used for thick films of salt solutions, and the unit of mol/L is used for the salt concentration.

Substituting Eq. [20] into Eqs. [5] to [7] gives

$$\frac{4C_{cr}}{h_{cr}{}^2 \upsilon R_g T}\left(\frac{\partial\sigma}{\partial C}\right)^2_{C=C_{cr}} - \frac{2\sigma}{R} - \frac{B}{h_{cr}{}^4} + 64000 C_{cr} R_g T \tanh^2\left(\frac{z\psi F}{4R_g T}\right)\exp(-\kappa h_{cr}) = 0 \qquad [22]$$

$$-\frac{8C_{cr}}{h_{cr}{}^3 \upsilon R_g T}\left(\frac{\partial\sigma}{\partial C}\right)^2_{C=C_{cr}} + \frac{4B}{h_{cr}{}^5} - 64000\kappa C_{cr} R_g T \tanh^2\left(\frac{z\psi F}{4R_g T}\right)\exp(-\kappa h_{cr}) = 0 \qquad [23]$$

$$\frac{24C_{cr}}{h_{cr}{}^4 \upsilon R_g T}\left(\frac{\partial\sigma}{\partial C}\right)^2_{C=C_{cr}} - \frac{20B}{h_{cr}{}^6} + 64000\kappa^2 C_{cr} R_g T \tanh^2\left(\frac{z\psi F}{4R_g T}\right)\exp(-\kappa h_{cr}) < 0 \qquad [24]$$

Equations [22] to [24] can be solved by applying a numerical technique. Using Matlab code developed by our team, Eqs. [22] to [24] are successfully solved simultaneously. The retarded Hamaker constant can be determined accurately by fitting the retarded van der Waals disjoining pressure, $\Pi = -B/h^4$, with the exact data of the Lifshitz theory and the full dielectric spectrum for water [1, 26], giving $B = 3.492\times10^{-29}$ J.m (The zero-frequency term in salt solutions of high concentration is negligibly small and is not considered here) [20]. As an example, NaCl is used for the numerical calculation of C_{cr} and h_{cr}. The numerical solutions obtained for films of NaCl solutions are $C_{cr} = 0.045$ mol/L and $h_{cr} = 25.626$ nm for R = 1.8 mm. The bubble radius of R = 1.8 mm is used as reported by Lessard and Zieminski [11]. The effect of bubble radius on the calculated critical concentration of NaCl is relatively weak. For example, for R = 1.8, 2 and 2.05 mm, the calculated critical concentrations of NaCl are 0.045, 0.043 and 0.042 mol/L, respectively. The concentration variation is within experimental errors. The additional experimental data needed in the calculation for NaCl solution films are as follows. The potential of the interface between air and NaCl solutions can be measured by microelectrophoresis using a Rank-Brothers zeta meter MK II (Rank Brothers Ltd, Cambridge, England) and fine air bubbles of 20 μm in diameter. Shown in Figure 2 are the experimental results (points) and the empirical approximation (line) for the modelling: $\psi = 1.097(\log C)^2 + 17.110\log C + 0.155$, where the units of potential and concentration are mV and mol/L, respectively. At 23 °C, Eq. [21] gives $\kappa = 3.239\sqrt{C}$, where the units of the Debye

constant and concentration are given in nm^{-1} and mol/L, respectively. As shown in Figure 3, the surface tension for NaCl solutions at 23 ^{o}C can be approximated by $\sigma = 0.0724 + 1.704 \times 10^{-3} C$, where the units for surface tension and concentration are N/m and mol/L, respectively.

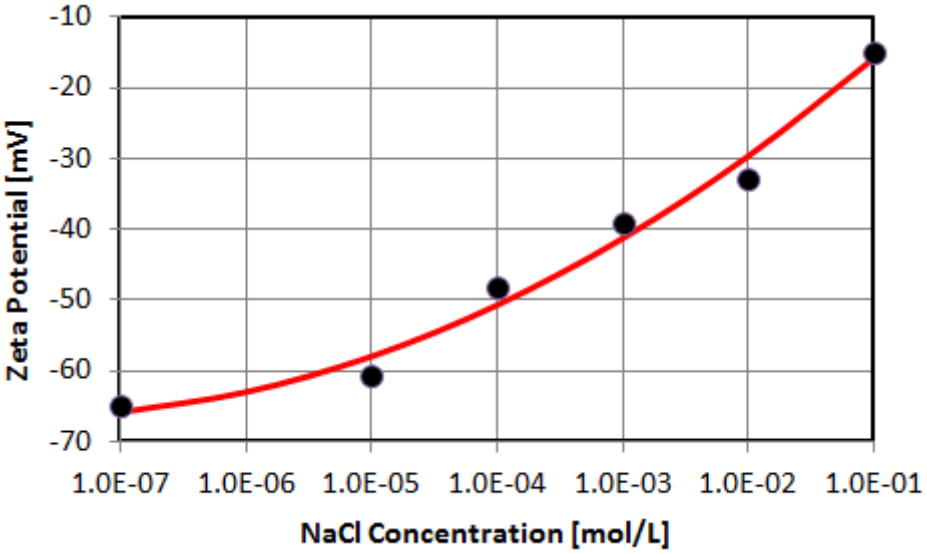

Figure 2. Zeta potential of air-NaCl interface versus NaCl concentration.

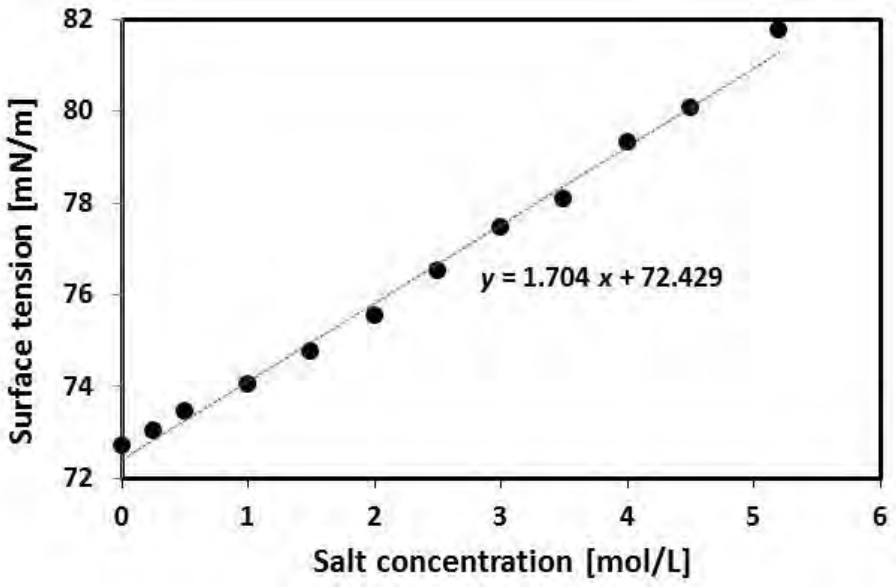

Figure 3. Surface tension of NaCl solutions versus concentration up to saturation at 23 ^{o}C [27].

The calculated result for $C_{cr} = 0.045\,\text{mol/L}$ is significantly different from the experimental results of 0.175 mol/L for NaCl solutions and for the bubble radius of 1.8 mm, as reported by Lessard and Zieminski [11]. The calculated result of $h_{cr} = 25.626\,\text{nm}$ is also too small compared with

the experimental results for salt solution films [28]. This significant difference indicates that there may be another attractive disjoining pressure, much stronger than the retarded van der Waals attraction, causing the film to rupture at larger thicknesses. Indeed, similar to the retarded van der Waals attraction, an empirical power-law dependence of hydrophobic attraction on thickness was reported for the foam films stabilized by surfactants [29]. Therefore, here we allow the force parameter B in Eqs. [22] - [24] to change and it is found that if $B = 52\times10^{-29}\,\text{J.m}$, the model gives the same results for $C_{cr} = 0.175\,\text{mol/L}$ as experimentally determined for NaCl. Evidently, the new force parameter is greater by an order of magnitude than $B = 3.492\times10^{-29}\,\text{J.m}$ for the retarded van der Waals attraction. The new critical thickness is equal to $h_{cr} = 50.302\,\text{nm}$, which is within the range of the available experimental results [28]. These new results show the weakness of the van der Waals attractions (which would cause the film rupture and bubble coalescence) in balancing the pressure of the Gibbs-Marangoni stress (which would inhibit the film rupture and bubble coalescence) at the experimental critical concentrations. In other words, to be able to predict the experimental critical concentration and thickness, strong attractive (other than van der Waals) disjoining pressures are required. This demands further investigation into nonDLVO (hydrophobic) intermolecular interactions [30].

4. CONCLUSIONS

In this paper we developed a novel methodology for predicting C_{cr}. We have shown that C_{cr} occurs at the local maximum of the pressure balance equation for capillary pressure, disjoining pressure and pressure of the Gibbs-Marangoni stress. We also showed that the previous simple predictions for C_{cr} could be obtained from our new, generic model described by Eqs. [5] - [7] when the van der Waals disjoining pressure is applied. We showed further that the hydration repulsive disjoining pressure could not be used to predict C_{cr} since the model equations have no solutions for C_{cr} and h_{cr} in this case, and the hydration repulsion is too short-ranged to affect the rupture of

aqueous films of salt solutions at larger thicknesses. We successfully used the new model to demonstrate the solution for C_{cr} and h_{cr} when the retarded Casimir-van der Waals disjoining pressure and the electrical double-layer disjoining pressure were applied. Comparing the new model with the experimental results for C_{cr} and h_{cr} for NaCl solutions, it showed that the retarded van der Waals disjoining pressure would not be strong enough to cause the film to rupture at high NaCl concentrations. Indeed, if a strong hydrophobic attraction is used in the model, the matching of the model results and the experimental data for C_{cr} for NaCl solutions is obtained, also giving a physically consistent solution for h_{cr}. The pressure constant of the power-law dependence of hydrophobic attraction on film thickness is greater, by an order of magnitude, than the Hamaker constant for the retarded van der Waals attraction. Further investigation to elucidate the role of hydrophobic attraction in determining C_{cr} and h_{cr} is needed.

AUTHOR INFORMATION

Corresponding Author

E-mail: anh.nguyen@eng.uq.edu.au. Phone: +61 7 336 53665. Fax: +61 7 336 54199.

Notes

The authors declare no competing financial interest.

ACKNOWLEDGEMENTS

The authors gratefully acknowledge the financial support from the Australian Research Council (Grant DP0985079). The assistance of Ms Kitty Tang in measuring the surface potential is warmly acknowledged.

REFERENCES

1. Nguyen, A. V.; Schulze, H. J. Colloidal Science of Flotation; Marcel Dekker: New York, 2004.
2. Leja, J. Surface Chemistry of Froth Flotation; Plenum Press: New York, NY, 1982.
3. Harvey, P. A.; Nguyen, A. V.; Evans, G., M. Influence of Electrical Double-Layer Interaction on Coal Flotation. *J. Coll. Interface Sci.* **2002,** *250 (2)*, 337-343.
4. Kracht, W.; Finch, J. A. Bubble Break-up and the Role of Frother and Salt. *Int. J. Miner. Process.* **2009,** *92* (3-4), 153-161.
5. Quinn, J. J.; Kracht, W.; Gomez, C. O.; Gagnon, C.; Finch, J. A. Comparing the Effect of Salts and Frother (Mibc) on Gas Dispersion and Froth Properties. *Miner. Eng.* **2007,** *20* (14), 1296-1302.
6. Kurniawan, A. U.; Ozdemir, O.; Nguyen, A. V.; Ofori, P.; Firth, B. Flotation of Coal Particles in Mgcl2, Nacl, and Naclo3 Solutions in the Absence and Presence of Dowfroth 250. *Int. J. Miner. Process.* **2011,** *98* (3-4), 137-144.
7. Bournival, G.; Pugh, R. J.; Ata, S. Examination of Nacl and Mibc as Bubble Coalescence Inhibitor in Relation to Froth Flotation. *Miner. Eng.* **2012,** *25* (1), 47-53.
8. Paulson, O.; Pugh, R. J. Flotation of Inherently Hydrophobic Particles in Aqueous Solutions of Inorganic Electrolytes. *Langmuir* **1996,** *12* (20), 4808-4813.
9. Nguyen, P. T.; Hampton, M. A.; Nguyen, A. V.; Birkett, G. The Influence of Gas Velocity, Salt Type and Concnetration on Transition Concentration for Bubble Coalescence Inhibition and Gas Holdup. *Chem. Eng. Res. Des.* **2012,** *90*, 33-39.
10. Marrucci, G.; Nicodemo, L. Coalescence of Gas Bubbles in Aqueous Solutions of Inorganic Electrolytes. *Chem. Eng. Sci.* **1967,** *22* (9), 1257-65.
11. Lessard, R. R.; Zieminski, S. A. Bubble Coalescence and Gas Transfer in Aqueous Electrolytic Solutions. *Ind. Eng. Chem. Fun.* **1971,** *10* (2), 260-9.
12. Craig, V. S. J.; Ninham, B. W.; Pashley, R. M. Effect of Electrolytes on Bubble Coalescence. *Nature* **1993,** *364* (6435), 317-19.
13. Hofmeier, U.; Yaminsky, V. V.; Christenson, H. K. Observations of Solute Effects on Bubble Formation. *J. Colloid Interface Sci.* **1995,** *174* (1), 199-210.
14. Christenson, H. K.; Bowen, R. E.; Carlton, J. A.; Denne, J. R. M.; Lu, Y. Electrolytes That Show a Transition to Bubble Coalescence Inhibition at High Concentrations. *J. Phys. Chem. C* **2008,** *112* (3), 794-796.
15. Marrucci, G. Theory of Coalescence. *Chem. Eng. Sci.* **1969,** *24* (6), 975-85.
16. Prince, M. J.; Blanch, H. W. Transition Electrolyte Concentrations for Bubble Coalescence. *AIChE J.* **1990,** *36* (9), 1425-9.
17. Chan, B. S.; Tsang, Y. H. A Theory on Bubble-Size Dependence of the Critical Electrolyte Concentration for Inhibition of Coalescence. *J. Colloid Interface Sci.* **2005,** *286* (1), 410-413.
18. Yaminsky, V. V.; Ohnishi, S.; Vogler, E. A.; Horn, R. G. Stability of Aqueous Films between Bubbles. Part 1. The Effect of Speed on Bubble Coalescence in Purified Water and Simple Electrolyte Solutions. *Langmuir* **2010,** *26* (11), 8061-8074.
19. Parkinson, L.; Ralston, J. The Interaction between a Very Small Rising Bubble and a Hydrophilic Titania Surface. *The Journal of Physical Chemistry C* **2010,** *114* (5), 2273-2281.

20. Firouzi, M.; Nguyen, A. V. On the Effect of Van Der Waals Attractions on the Critical Salt Concentration for Inhibiting Bubble Coalescence (Accepted). *Miner. Eng.* **2013**.

21. Pashley, R. M. Hydration Forces between Mica Surfaces in Electrolyte Solutions. *Adv. Colloid Interface Sci.* **1982,** *16*, 57-62.

22. Pashley, R. M. Hydration Forces between Mica Surfaces in Aqueous Electrolyte Solutions. *J. Colloid Interface Sci.* **1981,** *80* (1), 153-62.

23. Pashley, R. M.; Israelachvili, J. N. Dlvo and Hydration Forces between Mica Surfaces in Magnesium(2+), Calcium(2+), Strontium(2+), and Barium(2+) Chloride Solutions. *J. Colloid Interface Sci.* **1984,** *97* (2), 446-55.

24. Cevc, G.; Hauser, M.; Kornyshev, A. A. Effects of the Interfacial Structure on the Hydration Force between Laterally Nonuniform Surfaces. *Langmuir* **1995,** *11* (8), 3111-18.

25. Butt, H. J. Measuring Electrostatic, Van Der Waals, and Hydration Forces in Electrolyte Solutions with an Atomic Force Microscope. *Biophys. J.* **1991,** *60* (6), 1438-44.

26. Nguyen, A. V. Improved Approximation of Water Dielectric Permittivity for Calculation of Hamaker Constants. *J. Colloid Interface Sci.* **2000,** *229* (2), 648-651.

27. Ozdemir, O.; Karakashev, S. I.; Nguyen, A. V.; Miller, J. D. Adsorption and Surface Tension Analysis of Concentrated Alkali Halide Brine Solutions. *Min. Eng.* **2009,** *22* (3), 263-271.

28. Karakashev, S. I.; Nguyen, P. T.; Tsekov, R.; Hampton, M. A.; Nguyen, A. V. Anomalous Ion Effects on Rupture and Lifetime of Aqueous Foam Films Formed from Monovalent Salt Solutions up to Saturation Concentration. *Langmuir* **2008,** *24* (20), 11587-11591.

29. Wang, L.; Yoon, R.-H. Hydrophobic Forces in the Foam Films Stabilized by Sodium Dodecyl Sulfate: Effect of Electrolyte. *Langmuir* **2004,** *20* (26), 11457-11464.

30. Meyer, E. E.; Rosenberg, K. J.; Israelachvili, J. N. Recent Progress in Understanding Hydrophobic Interactions. *Proc. Natl. Acad. Sci. U. S. A.* **2006,** *103*, 15739-15746.

31. Henry, C. L.; Parkinson, L.; Ralston, J. R.; Craig, V. S. J. A Mobile Gas-Water Interface in Electrolyte Solutions. *J. Phys. Chem. C* **2008,** *112* (39), 15094-15097.

[&] It is noted that the bubble rise velocity is mainly affected by buoyancy which is significantly stronger than the effect of inorganic salts. The changes in boundary conditions affected by salts are too weak to be detected by changes in the bubble rise velocity [31]. Indeed, the boundary condition affected by salts can be probed by changes in the interfacial physics and intermolecular forces governing liquid film drainage between two approaching (colliding) bubbles. The important role of salts in thin liquid film drainage is discussed in the recent literature [31]: "We must acknowledge that there are differences between a single bubble rising in a quiescent fluid and the thinning of a film between two colliding bubbles. Diffusion of electrolyte from the bulk to the interface, which arrests any induced surface tension gradient, is likely to be different, particularly if the film is very thin.

Additionally, the presence of surface forces may influence the distribution of ions in a thin film". The transition from mobile to immobile air-water interfaces in salt solutions is established by experiments with colliding bubbles [19]. Immobile (no-slip) boundary condition at the film interface between air and KCl solutions is confirmed when the bubble approaches the solid surface. It is also confirmed that the bubbles terminal velocities in the same KCl solutions displays full slip boundary condition at the air-solution interface of air bubbles in KCl solutions. It is further suggested that a surface tension gradient can be established during drainage of a thin liquid film even in the case of very clean air-water interface [18]. Indeed, the radial plug flow in the thin liquid film results in a non-uniform ion distribution in the surface which leads to a surface tension gradient sufficiently large to alter the air-bubble interface from mobile to partially mobile or immobile interface. Evidently, the effect of salts on film drainage and instability is significant and cannot be contrasted by the bubble rise velocity.

TOC GRAPHIC

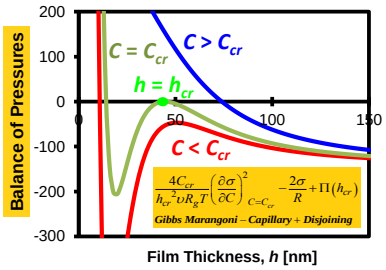
Balance of Pressures
200
100
0
-100
-200
-300
0
50
100
150
C = C_cr
C > C_cr
h = h_cr
C < C_cr
Gibbs Marangoni – Capillary + Disjoining
Film Thickness, h [nm]